RSC Advances

PAPER

View Article Online
View Journal | View Issue

Cite this: *RSC Adv.*, 2016, **6**, 83429

Structural modifications induced by an *in vitro* maturation process in zona pellucida glycoproteins of bovine oocytes. A Raman microspectroscopy analysis†

G. Rizo,‡[a] M. Roldán-Olarte,‡[a] D. C. Miceli,‡[a] L. E. Jiménez‡[b] and R. M. S. Álvarez‡*[b]

Oocyte quality is a determinant factor in the efficiency of an *in vitro* production process. Since the first oocyte–sperm interactions take place in the zona pellucida, the evaluation and characterization of this egg external matrix is of vital importance for the success of the *in vitro* fertilization process in mammals. Here we evaluate the modifications in the glycoproteins of the zona pellucida of bovine oocytes resulting from *in vitro* maturation. Using Raman microspectroscopy, subtle spectral differences were straightforwardly related to specific structural changes that could be correlated with known ultrastructural and morphological properties of the zona pellucida. We performed a detailed evaluation of features concerning both the protein backbone and the glycan moieties of the glycoproteins of the zona pellucida from immature and *in vitro* matured oocytes. Specific spectral differences involving amide I, amide III, and several bands belonging to the sugar residues allowed the characterization of these two stages in oocyte maturation. A molecular rearrangement of the glycoproteins consisting in the exposition of terminal sugar residues that play a key role in sperm recognition while the glycan core is covered by the polypeptide chain was derived from this study. These results demonstrate the efficiency of the Raman microspectroscopy technique to perform a biochemical characterization of the zona pellucida of bovine oocytes. This technique would be useful to discriminate between immature and *in vitro* matured oocytes and could also provide a basis for the understanding of the changes induced by maturation methods and of their impact on *in vitro* fertilization.

Received 9th March 2016
Accepted 24th August 2016

DOI: 10.1039/c6ra06243a

www.rsc.org/advances

Introduction

The *in vitro* embryo production (IVP) process represents a valuable resource for embryology research in mammals to solve reproductive problems and to conserve gametes of animals with high genetic value or at risk of extinction. However, in spite of scientific efforts to improve its performance, the IVP process is still lacking in efficacy. In cattle, this technique consists of three important stages: *in vitro* maturation of cumulus–oocyte complexes (COCs), *in vitro* fertilization (IVF), and *in vitro* culture of preimplantation embryos (IVC) in a synthetic medium. Since the efficiency of this biotechnological process is strongly dependent on oocyte quality, the first stage is particularly crucial, so the *in vitro* maturation process has been extensively studied in different mammalian species.

The oocyte maturation process is normally regarded as a series of either nuclear or cytoplasmic events, both of them essential to ensure the developmental competence of the oocyte and enable it to fully support fertilization and embryo development. However, it has been demonstrated that maturation of the extracellular matrix surrounding the mammalian egg cell, the zona pellucida (ZP), is also of vital importance for the success of fertilization since it is involved in several processes such as oogenesis, fertilization, preimplantation development, and early stage embryo protection.[1]

The ZP is a transparent envelope with a multilaminar structure.[1a] Depending on the species, it is made up of three or four highly glycosylated and sulfated glycoproteins assembled in a three dimensional ordered filament structure.[2] It has been reported that this external matrix serves as the primary sperm receptor and that the carbohydrate moieties of the ZP glycoproteins would be responsible for the sperm binding activity, although the precise mechanism for sperm–ZP interaction

[a]*Instituto Superior de Investigaciones Biológicas (INSIBIO), CONICET-Universidad Nacional de Tucumán (UNT), Instituto de Biología 'Dr Francisco D. Barbieri', Facultad de Bioquímica, Química y Farmacia, UNT, Chacabuco 461, T4000ILI – San Miguel de Tucumán, Argentina*

[b]*Instituto de Química del Noroeste Argentino (INQUINOA), CONICET-UNT, Instituto de Química Física, Facultad de Bioquímica, Química y Farmacia, UNT, San Lorenzo 456, San Miguel de Tucumán, T4000CAN, Tucumán, Argentina. E-mail: mysuko@fbqf.unt.edu.ar*

† Electronic supplementary information (ESI) available. See DOI: 10.1039/c6ra06243a

‡ G. R. and L. E. J. are grateful to CONICET for Doctoral Fellowships. M. R. O., D. C. M., and R. M. S. A. are career researchers of CONICET.

remains unclear.[3] In general, the heterogeneity of ZP glycoproteins in mammalian oocytes is due to the *O*- and *N*-linked oligosaccharide side chains rather than to the polypeptide portion.

In bovine oocyte, the ZP is composed of three glycoproteins called ZP2, ZP3 and ZP4.[4] In this species, the major neutral *N*-linked chain consists of only one structure, a high-mannose-type chain containing five mannose residues.[5] α-Mannosyl residues at non-reducing termini have proved to be essential for the sperm-binding activity of bovine ZP.[3b] Moreover, recent studies demonstrated that ZP3 interacts with ZP4 forming active complexes where the *N*-linked glycans bound to the hinge region are involved in sperm-binding.[6]

On the other hand, ultrastructural studies have shown that the overall ZP aspect is characterized by a fibrous network, with numerous meshes and holes. Besides, a clear correlation between the morphology of the ZP surface and the degree of oocyte maturity is revealed in the apparition of more compact areas around the holes.[7]

A close correlation between changes affecting ZP ultrastructure, morphology and chemical composition is needed to reach accurate knowledge of the mechanisms whereby mature oocytes become competent for fertilization and development. Raman microspectroscopy (RMS) is a particularly useful tool for this purpose since it provides a unique molecular fingerprint of the ZP macromolecules under physiological conditions without staining or fixing[8] as well as after fixation.[9] Although this powerful technique has been increasingly used for the study of single cells, only a few works have account for its application in the investigation of the biochemical composition of mammalian oocytes.[8–10]

The aim of the present work was to evaluate by RMS the effect of the *in vitro* maturation process on ZP glycoproteins of bovine oocytes. Specifically, we compared the Raman spectra obtained from the ZP of immature (IMM) and *in vitro* matured (IVM) oocytes. Since structural changes affecting either the protein backbone or the carbohydrate moiety of glycoproteins were expected to be manifested by specific Raman bands, the main spectral differences observed were interpreted in terms of conformational changes in the ZP components upon maturation. The spectral data were in agreement with previous results obtained by Scanning Electron Microscopy (SEM).[7b] The overall results here presented show the efficiency of the RMS technique to obtain a biochemical characterization of the ZP at the single cell level, providing a basis for the understanding of the changes induced by oocyte maturation methods and hence derive their impact on *in vitro* fertilization. Statistical analyses on specific spectral differences demonstrate the ability of RMS to discriminate between immature and *in vitro* matured bovine oocytes by a rapid assessment of the spectra of the ZP.

Experimental

Cumulus oocytes complexes (COCs) collection

Bovine ovaries were collected from young beef cows (*Bos taurus*) at a local abattoir and transported in sodium phosphate buffer (PBS), pH 7.4, at 37 °C for processing within 2 h after collection. For the present study, three different experiments were carried out. In each experiment, a pool of 20–30 ovaries from 10 to 15 heifers was employed. COCs were obtained by aspiration from follicles of 2 to 8 mm in diameter with an 18-gauge needle connected to a 5 ml disposable syringe containing ~1 ml of Tirodes Albumin Lactate Piruvate (TALP) medium supplemented with 10 mM *N*-2-hydroxyethylpiperazine-*N*′-2-ethanesulfonic acid (HEPES) plus 10% (v/v) fetal bovine serum (FBS, Internegocios, Buenos Aires, Argentina). Immature oocytes with uniform ooplasm with intact and compact cumulus cell layers were selected by stereoscopic microscope observation. After two washes in TALP–HEPES medium, COCs were randomly distributed into two groups; COCs in the first group were used for Raman measurements at the immature stage (IMM) and those in the second group were processed to obtain *in vitro* matured (IVM) COCs.

In vitro maturation

In each experiment, groups of 40 selected COCs were transferred to 4-well plates (Nunc, Rockslide, Denmark) containing 400 μl tissue culture medium (TCM)-199 (Gibco1150-059, Grand Island, NY, USA) supplemented with 10% (v/v) FBS, 0.05 IU ml^{-1} recombinant follicular stimulant hormone (rFSH, Puregon, Organon, Dublin, Ireland), 0.13 mmol l^{-1} of sodium pyruvate (Sigma P4562, St. Louis, MO, USA), 20 μM cysteamine (Sigma M9768) and 1% antibiotic–antimycotic solution (Gibco product 15240). COCs were cultured for 22 h at 38.5 °C under a 5% CO_2 atmosphere.[11]

Preparation of oocytes for Raman analysis

Cumulus cells of immature and *in vitro* matured COCs (Fig. 1A and B) were removed by pipetting in warm TALP–HEPES medium with 0.3 mg ml^{-1} hyaluronidase (Sigma Aldrich, UK) as previously described.[12] Only denuded IMM oocytes and denuded IVM oocytes in metaphase II (MII, showing the extrusion of the first polar corpuscle), were used in these experiments (Fig. 1C and D). Oocytes were washed three times with PBS and fixed for 30 minutes in 4% w/v paraformaldehyde solution.[9b] After fixation, oocytes were washed thrice in PBS and stored at 4 °C until Raman measurements.

Raman microspectroscopy measurements

The oocytes from the IMM ($n = 15$) and IVM ($n = 15$) groups were transferred individually to 5 μl drops of PBS on gold-coated sample slides. RMS measurements between 3500 and 50 cm^{-1} were performed with a DXR confocal Raman Microscope (Thermo Fisher Scientific) equipped with a 780 nm excitation wavelength at 24 mW of power (5 cm^{-1} spectral resolution). A confocal aperture of 50 μm slit was used for data collection. Samples were focused with a 20× objective.

In order to avoid oocyte dehydration caused by long irradiation periods, the maximum number of sampling points on the ZP of a single oocyte was 5 (Fig. 1E); however, depending on the resistance of each oocyte, in some cases spectra could be taken only from 3 or 4 different points. Each sampling point yielded one individual-spectrum, which was acquired by accumulating

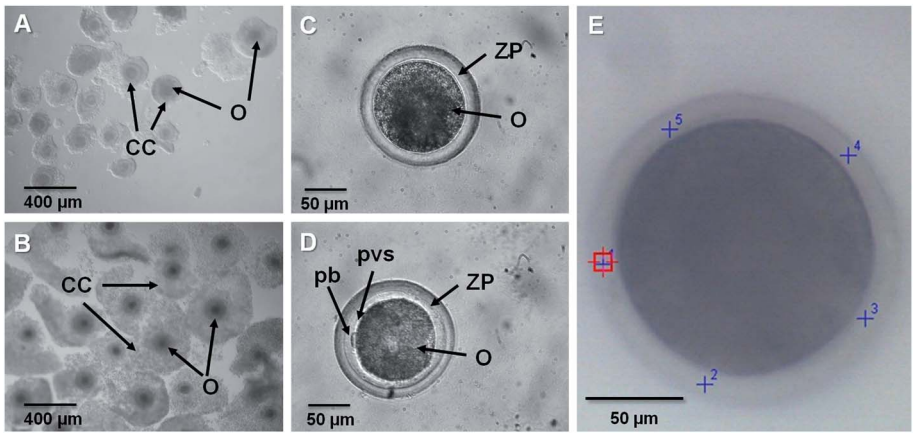

Fig. 1 Bovine cumulus oocytes complexes (COCs) and oocytes before and after *in vitro* maturation. (A) Immature (IMM) COCs and (B) *in vitro* matured (IVM) COCs, by using a stereo microscope (Olympus SZ51). (C) Denuded IMM oocyte and (D) denuded IVM oocyte, by using an inverted microscope (Zeiss Axiovert 25). (E) Bovine oocyte image obtained with a DXR confocal Raman microscope (Thermo Fisher Scientific) using a 20× objective. The maximum number of individual-spectra randomly located in the ZP of a single oocyte was 5, although for some oocytes only 3 or 4 spectra were obtained from different irradiation points. Note that IVM COCs show cumulus cells expansion (B) and a polar body (D). O: oocyte; CC: cumulus cells; pb: polar body; pvs: perivitelline space; + (in blue) indicates random points of laser irradiation in the ZP region for spectra measurement; □ (in red) displays the irradiation point at the time the image was captured.

60 expositions with an exposure time of 2 seconds each. All spectroscopic experiments were carried out at ambient temperature.

Data analysis and statistics

All spectral data were processed with the OMNIC 8 Software suite. A total 108 spectra were collected: 61 spectra corresponding to the immature oocyte group (IMM) and 47 spectra to the *in vitro* matured group (IVM). The spectral contribution of the PBS was subtracted from each spectrum and a subsequent baseline correction was individually applied to the spectral range comprised between 2100 and 600 cm^{-1} (see Fig. ESI1†). The spectral profile of most of the points sampled within a group of oocytes proved to be very similar to each other, allowing the generation of a single average-spectrum that

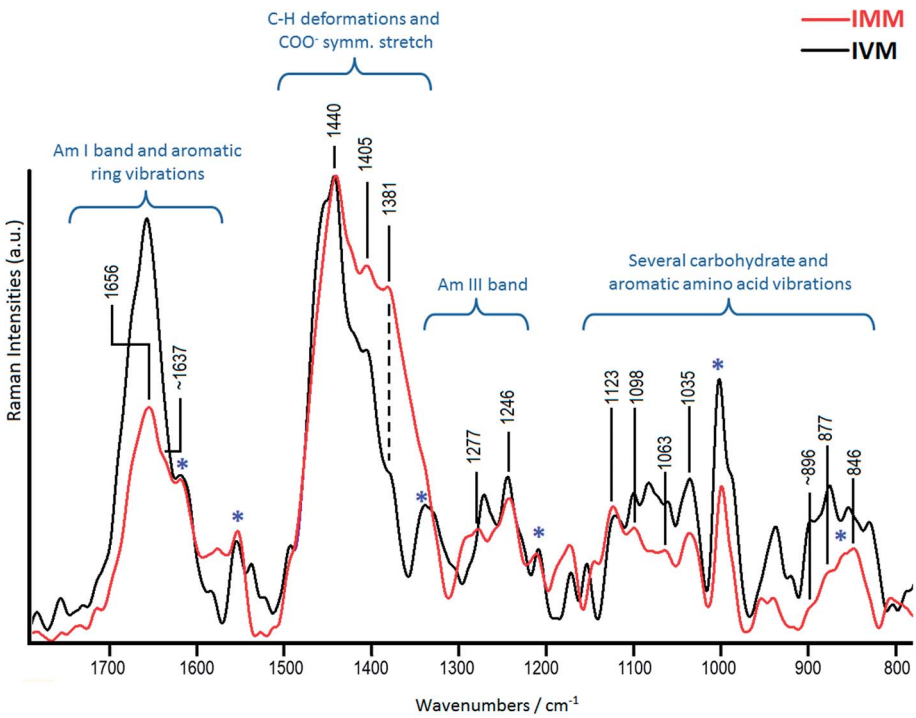

Fig. 2 Representative Raman average-spectra of the zona pellucida in immature (IMM) and *in vitro* matured (IVM) bovine oocytes. Spectral region comprising between 1800 and 800 cm^{-1} is shown. Bands associated to aromatic amino acid vibrations are denoted with *.

represents the overall spectral behavior of each oocyte group. These group-representative spectra were obtained by taking the arithmetic mean of the corresponding individual-spectra that showed little variation within a group. Thus, for the IMM group the average-spectrum was generated with 42 individual-spectra, while 39 spectra were used for obtaining the IVM average-spectrum. Then, both average-spectra were truncated to the 800–1800 cm^{-1} region for data analysis, as shown in Fig. 2.

In order to perform a detailed analysis of the changes induced by *in vitro* maturation in the protein structure, special attention was paid to the amide I (AmI, 1550–1750 cm^{-1}) and amide III (AmIII, 1200–1300 cm^{-1}) spectral regions, since the precise position and relative intensities of these bands indicate the presence of α-helixes, β-sheets, random coils, and turns conformations.[13] The overlapping components in these regions were mathematically decomposed using the GRAMS/32 software. The fitting result obtained using Voigt functions was visually evaluated by overlapping the reconstituted overall curve on the original spectra.

For statistical analysis we used the INFOSTAT program. A single ZP spectrum for each oocyte was obtained by averaging the corresponding 3, 4, or 5 individual-spectra recorded as described above. Thus, the statistical analysis was performed using a total of 30 spectra corresponding to 15 IMM and 15 IVM oocytes (see Table ESI1†). Taking into account the magnitude of the spectral differences between both groups of oocytes, two variables were chosen for the analysis: the relative intensities of the signals at ~1381 and ~1658 cm^{-1} with respect to the height of the band at ~1000 cm^{-1}, used as internal standard, (I_{1381}/I_{1000} and I_{1658}/I_{1000}, respectively). We used the *t*-test to compare their respective band intensities in the IMM and IVM groups. The discriminant analysis with the same variables was also performed to get the discriminant function.

Results and discussion

The analysis of most of the observed Raman features in the average-spectra for the ZP of IMM and IVM oocytes, shown in Fig. 2, is presented. Both domains of the glycoproteins constituting the bovine oocyte ZP are manifested in the Raman spectra: on one hand, the protein AmI and AmIII bands can be easily identified, together with several aromatic amino acids vibrations; on the other, various bands associated with carbohydrate chains and specific groups bound to saccharide residues such as sulfate and sialic acid can also be observed.

The vast literature related to the complex amide bands propitiates the following generalizations for protein conformations: α-helical domains contribute to the AmI and AmIII bands in the intervals between 1640–1655 and 1260–1310 cm^{-1}, respectively; β-sheet structures give the AmI band in the 1665–1680 cm^{-1} region and AmIII between 1230–1245 cm^{-1}; for irregular or disordered domains (random coils) the respective AmI and AmIII bands appear between 1655–1665 and 1245–1270 cm^{-1}; turns can be observed at 1680–1696 cm^{-1}. On the other hand, since most glycoproteins contain *N*-acetylglucosamine, *N*-acetylgalactosamine and sialic acid, their Raman spectra also exhibit the AmI (at 1632–1640 cm^{-1}) and AmIII bands (1330–1340 cm^{-1}) belonging to the amide group of these carbohydrate substituents.[14] In addition, the glycerol group normally gives a weak though well-defined Raman band at 873 cm^{-1} with a shoulder around 890 cm^{-1}, which is associated with the sialic acid of glycoproteins.[15] Other particularly interesting Raman bands of glycoproteins correspond to the sulfate substituents attached to the *N*-acetylglucosamine residues: the symmetric stretching of the OSO_3^- group, appearing as a strong band at *ca.* 1064 or 1079 cm^{-1} according to the orientation relative to the pyranose ring, and the symmetric and asymmetric stretching modes of the C–O–S linkage, observed between 977–995 and 820–853 cm^{-1}, respectively.[14a] Several well-characterized Raman bands in literature, belonging to vibrations of aromatic amino acids, were also assigned.

The following spectral regions were evaluated and spectral differences were sought in order to determine if the *in vitro* maturation process modifies the ZP components.

1500–1700 cm^{-1} region

This spectral region shows significant differences between both average-spectra, regarding not only their relative intensities but also their band contours. Thus, in the IMM spectrum the presence of several components is clearly observed, while the IVM spectrum shows a stronger and smoother band (see Fig. 2).

The shape of the strong band at 1658 cm^{-1} in the IVM spectrum is similar to that reported for matured mice oocytes where the maximum, also at 1658 cm^{-1}, has been assigned to the protein AmI mode and a shoulder observed at *ca.* 1620 cm^{-1} has been associated with the ring vibration of aromatic amino acids.[9b] The Raman and the second derivative spectra of matured ovine oocyte ZP has been also reported.[8] In that work the protein AmI band appeared as the main component at 1655 cm^{-1} while a weak component at 1640 cm^{-1} and two medium intensity components between 1620 and 1605 cm^{-1} were also shown but not assigned.[8] Here, we propose a complete assignment of the vibrational modes contributing to this spectral region in both the IVM and IMM spectra based on the deconvolution attempts presented in Fig. 3.

Six component bands fit well with the IMM contour comprised between 1600 and 1700 cm^{-1} (Fig. 3A). All these components were associated with the AmI mode, with the exception of the one at 1617 cm^{-1}, which was assigned to the Tyr ring stretching.[9b,16] The component at 1636 cm^{-1} was assigned to the AmI vibration belonging to the saccharide moiety,[14b] in agreement with the high *N*-acetylglucosamine content that characterizes the carbohydrate chains of the ZP glycoproteins.[17] Turns, β-sheets, random coils, and α-helixes protein conformations were assigned to the components at 1694, 1676, 1660, and 1649 cm^{-1}, respectively. Fig. 3B shows the component bands in the corresponding region of the IVM average-spectrum. Bands associated with the protein conformations remained almost unchanged with respect to those observed in the IMM average-spectrum, indicating that the overall protein secondary structure did not undergo detectable structural modifications with the *in vitro* maturation. However, a remarkable decrease in the intensity of the AmI of the

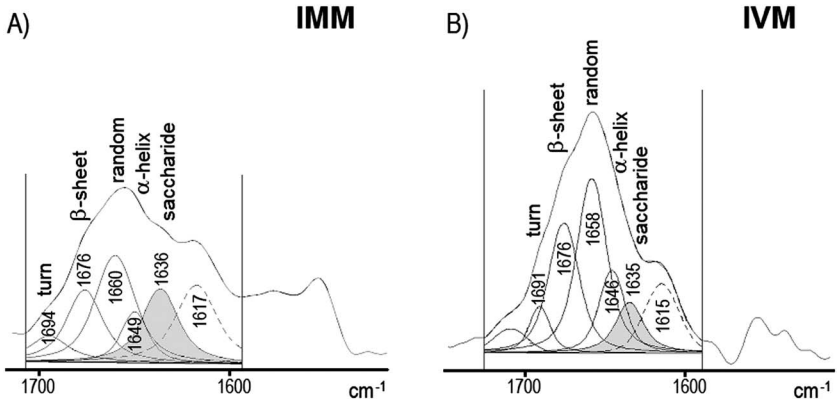

Fig. 3 Decomposition of the Raman spectra in the region corresponding to the amide I vibration of (A) zona pellucida of immature bovine oocytes (IMM) and (B) zona pellucida of *in vitro* matured bovine oocytes (IVM). The shaded band corresponds to the amide I mode of the saccharide moiety. The band indicated by the dashed line is assigned to the tyrosine (Tyr) ring stretching.

saccharide acetamide group (1635 cm^{-1}) was estimated by the peak fitting procedure, which is consistent with the smoother band shape in the IVM spectrum.

1350–1500 cm^{-1} region

The IMM Raman spectrum shows several intense bands in this spectral region (Fig. 2). Most of these features correspond to C–H deformations of both the protein and the glycan moieties: the strongest band of the IMM spectrum, located at 1440 cm^{-1}, together with the shoulder at 1424 cm^{-1} approximately, were assigned to the CH_2/CH_3 deformations of the peptide backbone,[13d] while the band at 1381 cm^{-1} was assigned to the CH_3 deformation mode of the acetamide groups attached to the sugar residues.[14a,15] Although these C–H deformation bands do not supply structural information, significant spectral differences involving the carbohydrates vibrations could be found when the ZP spectra of IMM and IVM oocytes were compared: in the IVM spectrum, the protein CH_2/CH_3 band (1441 cm^{-1}) is still the dominant band but the acetamide CH_3 band of carbohydrate chains has experienced a remarkable intensity decrease, becoming a shoulder of medium/weak intensity. The behavior of this acetamide band makes it suitable for discriminant analysis between both oocyte developmental stages, as will be discuss later. In addition, the strong feature at 1405 cm^{-1} in both spectra was assigned to the symmetric vibration of the COO^- group of the *N*-acetylneuraminic residues, in agreement with previous studies of glycosaminoglycans, where the COO^- symmetric stretching was reported at 1411 cm^{-1} for of the glucoronate residue and at 1405 cm^{-1} for the glycosides of *N*-acetylneuraminic acid.[14a,15]

1200–1350 cm^{-1} region

The AmIII vibration is expected in this spectral region. Various weak and overlapping bands can be observed between 1290 and 1210 cm^{-1} in the IMM spectrum (Fig. 2). Upon deconvolution, other additional components are solved, as shown in Fig. 4A. Decomposed bands at 1277, 1246, and 1237 cm^{-1} were tentatively assigned to the AmIII of α-helix, random coil, and β-sheet protein conformations, respectively, according to the reported values in the literature.[13b,13d,18] Other weak bands belonging to vibrations located in the saccharide moiety are also expected in this region, such as the asymmetric stretching mode of the OSO_3^- group that was reported at 1269 cm^{-1} for sulfate glycosaminoglycans[14a] and the CH_2OH deformation of methyl glycoside sialosides appearing at 1224 and 1284 cm^{-1}.[15] Consequently, an ambiguous assignment cannot be ruled out. The AmIII mode belonging to the carbohydrate moiety is expected around 1330 cm^{-1}, based on results reported for *N*-acetyl-monosaccharides (1327–1340 cm^{-1}) and glycosides of *N*-acetylneuraminic acid (1330 cm^{-1});[14a,15] however, the presence of this band is barely detected in the IMM spectrum. The ZP spectrum of IVM oocytes shows the region corresponding to the protein AmIII mode exhibiting two broad bands, with maxima at 1272 and 1244 cm^{-1} and a shoulder at ~1232 cm^{-1} (Fig. 2 and 4B) which were assigned to α-helix, random coil, and β-sheet conformations, respectively, in agreement with the features observed in the IMM spectrum. In addition, this protein AmIII assignment is in line with the behavior observed for the AmI bands since (i) not significant changes in the protein secondary structure were detected upon *in vitro* maturation and (ii) both amide bands indicate that the prevailing conformation in ZP glycoproteins is a random coil. The IVM spectrum shows a broad band with maximum at 1339 cm^{-1} and a shoulder at 1330 cm^{-1} approximately, which are suitable to be assigned to the AmIII mode of carbohydrates and the $C–C_\alpha–H$ deformation of the protein backbone. This last mode is typical of an α-helix conformation and was reported at 1345 cm^{-1} for human serum albumin, ferritin and glutathione transferase.[13d]

800–1200 cm^{-1} region

In general, the main spectral features of carbohydrate chains are the coupled C–O stretching with the C–O–H deformation modes, observed as a triplet of peaks at 1025–1045, 1080–1100, and 1110–1152 cm^{-1}.[5,14a] In our spectra, this three bands pattern appears distorted due to the presence of additional bands corresponding to the symmetric stretching vibration of

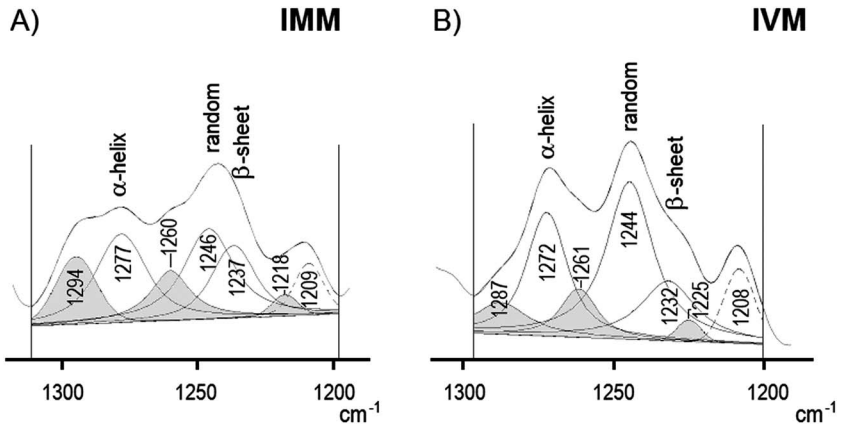

Fig. 4 Decomposition of the Raman spectra in the region corresponding to the protein amide III vibration of (A) zona pellucida of immature bovine oocytes (IMM) and (B) zona pellucida of *in vitro* matured bovine oocytes (IVM). The shaded bands are attributed to vibrations of the saccharide moiety. The band at 1209 cm (IMM)/1208 cm^{-1} (IVM) is assigned to an aromatic ring vibration (dashed line).

the OSO_3^- group, which was observed around 1060 and 1080 cm^{-1} in sulfated glycosaminoglycans[14a] (Fig. 2). In IMM spectrum, the bands at 1035, 1098, and 1123 cm^{-1} were assigned to the C–OH complex vibrations of the sugar residues, while the lower intensity features at 1063 and ~1079 cm^{-1} were attributed to the sulfate group. Upon *in vitro* maturation, the spectral profile of this region shows an intensification of the OSO_3^- stretching, particularly of the feature at 1081 cm^{-1}. This behavior was attributed to a change in the sulfate environment of IVM glycoproteins based on the wavenumbers reported for a different position/orientation of the OSO_3^- group with respect to the pyranose ring.[14a]

At lower wavenumbers, both IMM and IVM spectra show a doublet with maxima centered at 896/877 cm^{-1} which was attributed to the glycerol group of the sialic acid residues in agreement with reported data[14b] (Fig. 2).

In addition to the vibrations located in the glycan portion of ZP glycoproteins, well-characterized aromatic amino acid bands can be also observed in this spectral region: (i) the strong sharp band at 999 cm^{-1} (IMM) and 1001 cm^{-1} (IVM), typical of the in-plane-ring deformation of the Phe residues; normally this band is accompanied by one less intense band at 1030 cm^{-1},[13b,18a,19] which in our spectra is overlapped by the C–OH deformation at 1035 cm^{-1}. The Phe band at ~1000 cm^{-1} is particularly useful since it has proved to be insensitive to conformations or microenvironment and therefore it is suitable to be used as an internal standard.[20] In the IVM average-spectrum, this band exhibits a well-defined shoulder at 988 cm^{-1} approximately, which was attributed to the symmetric C–O–S stretching mode in agreement with the behavior reported for sulfated glycosaminoglycans.[14a] (ii) The characteristic Fermi doublet of Tyr residues can also be observed in the IVM average-spectrum, appearing at 829/854 cm^{-1}; in the IMM average-spectrum, this doublet is obscured by overlapping with the asymmetric stretching of the C–O–S linkage, reported between 820 and 850 cm^{-1} for glycosaminoglycans.[14a]

Table 1 lists the proposed assignments for the bands observed in the IMM and IVM average-spectra. The comparative analysis shows that the major spectral differences involve the glycan portion of the ZP glycoproteins, while no significant conformational changes in the polypeptide chain are detected. The total overlapping of the AmI band of the sugar moiety and the marked decrease in the intensity of the CH_3 deformation

Table 1 Raman bands of IMM and IVM spectra. A tentative assignment is proposed[a]

IMM	MIV	Assignment
1656 s	1658 vs	Protein AmI
~1637 sh		Saccharide AmI
1617 m	1617 m	Ar stretch.
1577 m	1584 w	Ar stretch.
1554 m	1553 m	Ar stretch.
	1452 sh	Protein CH_2/CH_3 def.
1440 vs	1441 vs	Protein CH_2/CH_3 def.
1424 sh	1419 sh	Protein CH_2/CH_3 def.
1405 vs	1405 s	COO^- symmetric stretch.
1381 s	~1381 sh	Saccharide protein CH_2/CH_3 def.
~1340 sh	1339 m	C–C_α–H def.
	~1330 sh	Saccharide AmIII
~1290 sh		Saccharide CH_2OH def.
1277 m	1272 m	Protein AmIII
1246 m	1244 m	Protein AmIII
	~1232 sh	Protein AmIII
1209 w	1208 w	Ar def.
1123 m	1120 m	Saccharide C–O–H stretch./def.
1098 m	1099 m	Saccharide C–O–H stretch./def.
~1079 sh	1082 m	OSO_3^- stretch.
1063 w	1060 m	OSO_3^- stretch.
1035 m	1035 m	Saccharide C–O–H stretch./def.
999 s	1001 s	Ar def. (Phe)
	988 s	C–O–S symmetric stretch.
~896 sh	896 m	Glycerol def.
877 w	877 m	Glycerol def.
~859 sh	854 m	Tyr
846 w		C–O–S asymmetric stretch.
	829 m	Tyr

[a] AmI: amide I; AmIII: amide III; Ar: aromatic; s: strong; m: medium; w: weak; sh: shoulder; stretch.: stretching; def.: deformation; Phe: phenylalanine; Tyr: tyrosine.

bands of the *N*-acetyl group suggest a rearrangement of the ZP glycoproteins occurring upon the *in vitro* maturation, so that the glycan core is covered by the polypeptide chains while the terminal sialic acid and sulfated residues remain exposed. This assertion is supported on one hand by the well-defined shoulder at 988 cm^{-1}, attributed to the C–O–S stretching and the intensification and upshift of bands associated with the sulfate group of glycans, observed in the IVM average-spectrum, and on the other, by the bands belonging to the sialic acid residue that remain observable and well defined, suggesting that they were not shielded by the polypeptide chains in the *in vitro* matured oocyte.

Characterizations by HPLC and ^{1}H-NMR spectroscopy had shown that 77% of the bovine ZP glycoproteins are made up of acidic carbohydrate chains. These acidic chains contain sialic acid at the non-reducing ends of *N*-acetyllactosamine repeats and sulfate groups at the C6 position of GlcNAc residues of the repeats.[5] Later, chemical and cytochemical analyses and sperm binding competition assays not only revealed that bovine ZP glycoproteins contain mainly Neu5Ac (84.5%) and Neu5Gc (15.5%) but also that the Neu5Ac(α-2-3)Gal(β1-4)GlcAc sequence is involved in the sperm–ZP interaction; besides, the presence of a specific receptor for α-2-3 linked sialic acid has been detected in bovine sperm.[3a] All these results support our proposed assignment of the Raman bands.

Furthermore, a previous structural analysis has also shown that the glycoconjugate distribution changes during oocyte maturation[21] and a model that accounts for the egg–sperm recognition process has been proposed based on a modification of the ZP structure by the cleavage of the ZP2 glycoprotein from a 3-D matrix but with no loss of zona components.[22] In addition, a subsequent study by scanning electron microscopy at high resolution has shown the three-dimensional structure of the ZP as a delicate meshwork of thin interconnected filaments, from which the existence of a correlation between ZP structure, function, and oocyte maturation stage has been derived.[7b] Thus, a "spongy" or "compact" appearance of the ZP has been considered as a consequence of the prevalence of different arrangements of microfilament networks according to the maturation stage of the oocyte.[7b] Consequently, our interpretation of the spectral changes revealed by the comparison between the ZP of immature and *in vitro* matured oocytes is strongly supported by the reported data.

Statistical analysis was performed by taking into account the bands corresponding to the protein AmI vibration and the CH_3 deformation of the acetamide groups in the glycan moiety. The election of these two bands to reflect the oocyte maturation state was based on the fact that the major spectral differences between the IMM and IVM average-spectra are given by the relative intensities of these two features (see Fig. 2). In order to make their peak heights comparable among all the spectra obtained in this study, the ~1000 cm^{-1} Phe band was used as an internal standard (see Table ESI1†). Fig. 5 represents these intensity ratios (I_{1381}/I_{1000} and I_{1658}/I_{1000}) extracted from the spectra generated for each oocyte by averaging the 3, 4, or 5 corresponding individual-spectra. Data extracted from IMM oocytes (represented by circles) show high intensity ratios of the

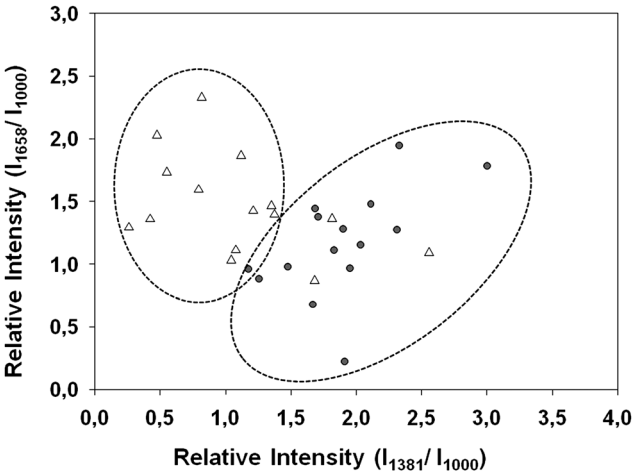

Fig. 5 Scatter plot of the relative intensities of the bands at 1381 and 1658 cm extracted from the ZP spectra of IMM (immature: $n = 15$) and IVM (*in vitro* matured: $n = 15$) oocytes. Relative intensities were obtained by calculating the peak height ratio of each band to the Phe band at ~1000 cm^{-1}. Separation of immature and *in vitro* matured oocytes can be observed along both axes mainly determined by the 1381 cm^{-1} band. Grey circle: IVM oocyte; triangle: IMM oocyte.

CH_3 deformation band and lower ratios for AmI bands. Most of the data corresponding to the IVM oocytes (represented by triangles) show an opposite behavior, being remarkable the intensity decrease of the CH_3 band. This representation indicates that the variable corresponding to the intensities of the glycan acetamide band (~1381 cm^{-1}) can be considered as a good spectral marker to differentiate between immature and *in vitro* matured oocytes.

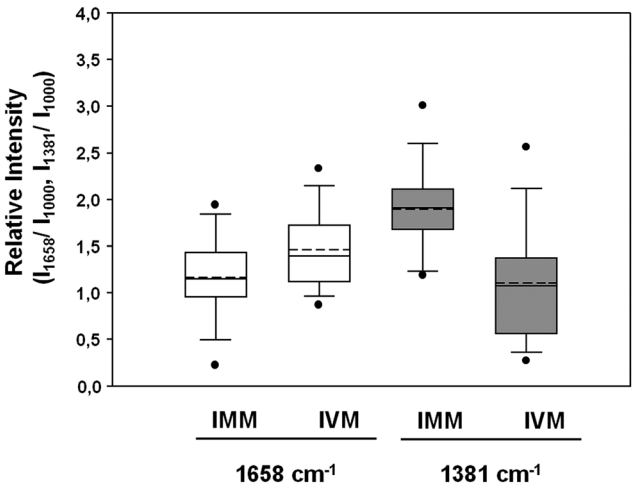

Fig. 6 Box-plot showing the average of Raman intensities obtained from ZP of IMM (immature: $n = 15$) and IVM (*in vitro* matured: $n = 15$) oocytes. Intensity ratios of bands at 1658 and 1381 cm^{-1} with respect to the Phe band at ~1000 cm^{-1} were separately analyzed. Within each box-plot, a dashed line shows the median, while the upper and lower lines indicate the first and third quartiles. Black circles are considered outliers. Significant differences between IMM and IVM oocytes were detected only for the 1381 cm^{-1} band ($p < 0.001$). White: 1658 cm^{-1} band; grey: 1381 cm^{-1} band.

The relative intensity of the CH_3 band found with the *t*-test indicates that this variable is different enough between both groups ($p < 0.001$), while the relative intensity of the AmI band is non-statistically different between IMM and IVM ($p = 0.057$). Fig. 6 compares the arithmetic mean of these I_{1381}/I_{1000} and I_{1658}/I_{1000} variables in the IMM and IVM groups, and evidences the statistically significant difference of the relative intensity of the CH_3 deformation band between both maturational states.

Discriminant analysis was performed by using the same variables. The standard coefficients calculated were 0.90 and −0.44 for I_{1381}/I_{1000} and I_{1658}/I_{1000}, respectively. The higher standard coefficient obtained for the CH_3 mode confirms the feasibility of this variable to differentiate between immature and *in vitro* matured oocytes. In addition, the discriminant function derived from the analysis allows the classification of an oocyte as immature – when the function value is positive or close to +0.82 – or as *in vitro* matured – when the function is negative or close to −0.82. Despite the low number of samples used in this analysis, a bovine oocyte can be classified as immature with 93.33% certainty, and as *in vitro* matured with of 80% certainty (see Fig. 5).

These results demonstrate the effectiveness of MRS as an alternative method to identify *in vitro* matured oocytes, based on the simple assessment of the deformation CH_3 band around 1380 cm^{-1} in the ZP spectra. Fig. 7 shows three different average-spectra corresponding to IVM oocytes. According to the similarities and differences among the overall spectral profiles, the 47 individual-spectra acquired for the *in vitro* matured oocytes were divided into three subgroups: the main subgroup, named IVM average-spectrum is composed of 39 individual-spectra, as stated in the Experimental section; the other two subgroups, named as IVM-SubG1 and IVM-SubG2, are composed of 4 individual-spectra each. Spectra in IVM-SubG1 and IVM-SubG2 show relatively high intensities of the band associated with the acetamide CH_3 deformation of carbohydrate chains that, according to the statistical analysis, is a behavior characteristic of immature oocytes (see Fig. 5). Our results are in agreement with previous reported data concerning the efficiency of the *in vitro* maturation process (86.7–90.0%)[23] as well the *in vitro* fertilization, in terms of cleavage rates (around 76.9%).[11]

Conclusions

The analysis of several well-characterized Raman features concerning both the protein and the glycan moieties of the ZP glycoproteins from IMM and IVM bovine oocytes is presented in this work. RMS is shown as a suitable technique to evaluate the ZP developmental stage, since the observed spectral differences were duly associated with molecular reorganizations. Specifically, the fact that the sialic acid residues involved in the sperm binding activity remain exposed while the rest of the carbohydrate chains are shielded by the protein domain allows us to infer the existence of a structural rearrangement produced by

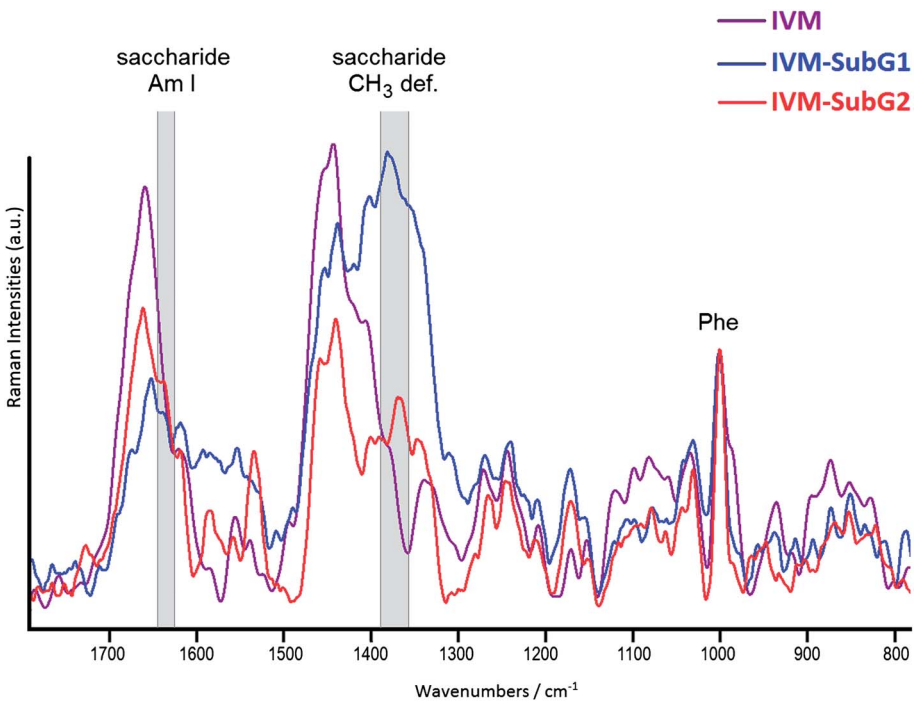

Fig. 7 Comparison between three different spectral profiles obtained from the ZP of 15 oocytes subjected to the *in vitro* maturation process. IVM-SubG1 and IVM-SubG2 are composed of 4 individual-spectra each, while IVM spectrum is composed of 39 individual-spectra. Amplification factors of 8 and 9 were used for the IVM-SubG1 and IVM-SubG2 spectra, respectively. The relative high intensity of the acetamide CH_3 deformation band observed in IVM-SubG1 and IVM-SubG2 suggests that some oocytes belonging to the IVM group are not mature. Note that the band attributed to the AmI vibration of saccharides, typically appearing as a well-defined shoulder in the spectra of immature oocytes, is also evidenced in the IVM-SubG1 and IVM-SubG2 spectra.

oocyte maturation. Although fixed oocytes were used in this work, the spectral analysis here presented contributes to the integration of previous data concerning ZP chemical conformation and oocyte surface morphology with structural and functional modifications according to the oocyte developmental stage. In addition, statistical analysis revealed that the CH_3 deformation band of the sugar acetamide groups can be considered as a spectral marker for discrimination between immature and *in vitro* matured oocytes. Consequently, the method used as a preliminary test can be extended to the assessment of the effects produced on the biochemical structure of ZP by different experimental media normally used during *in vitro* maturation; this knowledge could be useful to understand the response of *in vitro* matured oocytes to *in vitro* fertilization.

Acknowledgements

The authors would like to thank Calchaquí and Industrial del Norte S.A. slaughterhouses, Tucumán, Argentina, for providing the biological material. Special thanks are extended to Lic. Doly Chemes for her technical assistance during Raman measurements, to Dr Daniel Barrera for his controbution in the IVM processing, and to Mg. Lidia Benítez for her assistance in statistical analysis. All authors read and approved the final article.

References

1 (*a*) P. M. Wassarman, *J. Biol. Chem.*, 2008, **283**, 24285–24289; (*b*) G. F. Clark, *Syst. Biol. Reprod. Med.*, 2010, **56**, 349–364.

2 (*a*) C. Barros, J. A. Crosby and R. D. Moreno, *Cell Biol. Int.*, 1996, **20**, 33–39; (*b*) J. D. Harris, D. W. Hibler, G. K. Fontenot, K. T. Hsu, E. C. Yurewicz and A. G. Sacco, *DNA Sequence*, 1994, **4**, 361–393.

3 (*a*) J. G. Velasquez, S. Canovas, P. Barajas, J. Marcos, M. Jimenez-Movilla, R. G. Gallego, J. Ballesta, M. Aviles and P. Coy, *Mol. Reprod. Dev.*, 2007, **74**, 617–628; (*b*) K. Takahashi, K. Kikuchi, Y. Uchida, S. Kanai-Kitayama, R. Suzuki, R. Sato, K. Toma, M. Geshi, S. Akagi, M. Nakano and N. Yonezawa, *Biomolecules*, 2013, **3**, 85–107.

4 S. Noguchi, N. Yonezawa, T. Katsumata, K. Hashizume, M. Kuwayama, S. Hamano, S. Watanabe and M. Nakano, *Biochim. Biophys. Acta*, 1994, **1201**, 7–14.

5 T. Katsumata, S. Noguchi, N. Yonezawa, M. Tanokura and M. Nakano, *Eur. J. Biochem.*, 1996, **240**, 448–453.

6 K. Suzuki, N. Tatebe, S. Kojima, A. Hamano, M. Orita and N. Yonezawa, *Biomolecules*, 2015, **5**, 3339–3353.

7 (*a*) H. Suzuki, X. Yang and R. H. Foote, *Mol. Reprod. Dev.*, 1994, **38**, 421–430; (*b*) G. Familiari, M. Relucenti, R. Heyn, G. Micara and S. Correr, *Microsc. Res. Tech.*, 2006, **69**, 415–426.

8 L. Bogliolo, S. Ledda, P. Innocenzi, F. Ariu, D. Bebbere, I. Rosati, G. G. Leoni and M. Piccinini, *Cryobiology*, 2012, **64**, 267–272.

9 (*a*) B. R. Wood, T. Chernenko, C. Matthaus, M. Diem, C. Chong, U. Bernhard, C. Jene, A. A. Brandli, D. McNaughton, M. J. Tobin, A. Trounson and O. Lacham-Kaplan, *Anal. Chem.*, 2008, **80**, 9065–9072; (*b*) B. Davidson, A. A. Murray, A. Elfick and N. Spears, *PLoS One*, 2013, **8**, e67972.

10 (*a*) L. Bogliolo, O. Murrone, G. Di Emidio, M. Piccinini, F. Ariu, S. Ledda and C. Tatone, *J. Assist. Reprod. Genet.*, 2013, **30**, 877–882; (*b*) F. Liu, Y. Zhu, Y. Liu, X. Wang, P. Ping, X. Zhu, H. Hu, Z. Li and L. He, *Fertil. Steril.*, 2013, **99**, 684–689.

11 E. V. Garcia, D. C. Miceli, G. Rizo, P. A. Valdecantos and A. D. Barrera, *Theriogenology*, 2015, **84**, 589–599.

12 D. C. Garcia, D. C. Miceli, G. Rizo, E. V. Garcia, P. A. Valdecantos and M. Roldan-Olarte, *Zygote*, 2015, 1–6.

13 (*a*) T. Miura and G. J. Thomas Jr, *Subcell. Biochem.*, 1995, **24**, 55–99; (*b*) J. T. Pelton and L. R. McLean, *Anal. Biochem.*, 2000, **277**, 167–176; (*c*) M. M. Apetri, N. C. Maiti, M. G. Zagorski, P. R. Carey and V. E. Anderson, *J. Mol. Biol.*, 2006, **355**, 63–71; (*d*) A. Rygula, K. Majzner, K. M. Marzec, A. Kaczor, M. Pilarczyka and M. Baranska, *J. Raman Spectrosc.*, 2013, **44**, 1061–1076.

14 (*a*) R. Bansil, I. V. Yannas and H. E. Stanley, *Biochim. Biophys. Acta*, 1978, **541**, 535–542; (*b*) V. Oleinikov, M. Kovner, M. A. Ermishov, A. Tuzikov, N. Bovin and I. Nabiev, *Spectroscopy of Biological Molecules: New Directions*, 1999, pp. 331–332.

15 V. Oleinikov, E. Kryukov, M. Kovner, M. Ermishov, A. Tuzikov, S. Shiyan, N. Bovin and I. Nabiev, *J. Mol. Struct.*, 1999, **480–481**, 475–480.

16 J. M. Calafell, C. Nogues, M. Ponsa, J. Santalo and J. Egozcue, *J. Assist. Reprod. Genet.*, 1992, **9**, 365–372.

17 (*a*) M. Jimenez-Movilla, M. Aviles, M. J. Gomez-Torres, P. J. Fernandez-Colom, M. T. Castells, J. de Juan, A. Romeu and J. Ballesta, *Hum. Reprod.*, 2004, **19**, 1842–1855; (*b*) M. J. Izquierdo-Rico, M. Jimenez-Movilla, E. Llop, A. B. Perez-Oliva, J. Ballesta, R. Gutierrez-Gallego, C. Jimenez-Cervantes and M. Aviles, *J. Proteome Res.*, 2009, **8**, 926–941.

18 (*a*) H. Fabian and P. Anzenbacher, *Vib. Spectrosc.*, 1993, **4**, 125–148; (*b*) P. Monti, R. Simoni, R. Caramazza and A. Bertoluzza, *Biospectroscopy*, 1998, **4**, 413–419.

19 B. Ravikumar, R. K. Rajaram and V. Ramakrishnan, *J. Raman Spectrosc.*, 2006, **37**, 8.

20 B. Hernández, F. Pflüger, S. G. Kruglik and M. Ghomi, *J. Raman Spectrosc.*, 2013, **44**, 827–833.

21 (*a*) T. Rankin, P. Talbot, E. Lee and J. Dean, *Development*, 1999, **126**, 3847–3855; (*b*) T. L. Rankin, M. O'Brien, E. Lee, K. Wigglesworth, J. Eppig and J. Dean, *Development*, 2001, **128**, 1119–1126.

22 T. L. Rankin, J. S. Coleman, O. Epifano, T. Hoodbhoy, S. G. Turner, P. E. Castle, E. Lee, R. Gore-Langton and J. Dean, *Dev. Cell*, 2003, **5**, 33–43.

23 E. Dovolou, I. E. Messinis, E. Periquesta, K. Dafopoulos, A. Gutierrez-Adan and G. S. Amiridis, *Reprod. Domest. Anim.*, 2014, **49**, 665–672.